All Donor Electrochromic Polymers Tunable across the Visible Spectrum via Random Copolymerization

Dylan T. Christiansen,[†] Shunsuke Ohtani,[‡] Yoshiki Chujo,[‡] Aimée L. Tomlinson,[§] and John R. Reynolds*,[†]

[†]School of Chemistry and Biochemistry, School of Materials Science and Engineering, Center for Organic Photonics and Electronics, and Georgia Tech Polymer Network, Georgia Institute of Technology, Atlanta, Georgia 30332, United States

[‡]Department of Polymer Chemistry, Graduate School of Engineering, Kyoto University, Katsura, Nishikyo-ku, Kyoto 615-8510, Japan

[§]Department of Chemistry/Biochemistry, University of North Georgia, Dahlonega, Georgia 30597, United States

S *Supporting Information*

ABSTRACT: A series of conjugated, random terpolymers based on all donor repeat units are prepared via direct (hetero)arylation polymerization yielding cathodically colored electrochromic polymers that span the visible spectrum. The polymers are based on repeat units of a dialkylthiophene, a 3,4-propylenedioxythiophene, and dimers of 3,4-ethylenedioxythiophene. Using a tight feedback loop between computational and experimental chemistry, the colors of these polymers are controllably tuned to cover the visible spectrum by controlling the monomer ratios. Examinations via ultraviolet−visible−near-infrared spectroscopy, differential pulse voltammetry, spectroelectrochemistry, and colorimetry show that, while these systems can vary greatly in their spectral properties, their oxidation potentials are all low (<0.5 V vs Ag/AgCl). The color tunability allows for access to neutral state orange, red, pink, magenta, purple, and blue polymers of various hues with $a*$ values ranging from 22 to 35 and $b*$ values ranging from −44 to 45, while maintaining highly transmissive oxidized states. This approach allows access to a wide gamut of colors with only three monomers while affording materials with low oxidation potentials and high contrast.
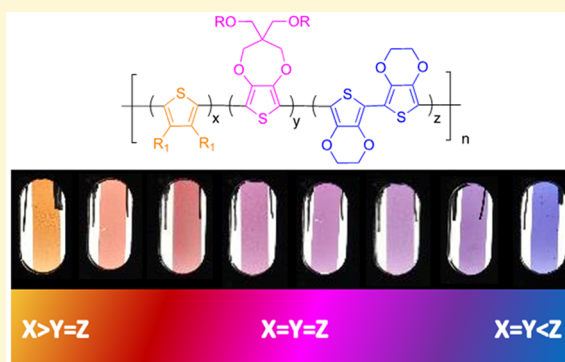
INTRODUCTION

The history of research of fully conjugated cathodically colored electrochromic polymers (ECPs) has yielded materials that span the entire color palette.[1−7] These polymers can be spray cast to form vividly colored films that upon oxidation become highly transmissive in the visible region. Methods of creating the wide range of possible colors involve incorporating numerous monomers in well-defined sequences. Random copolymerization has been used in many approaches as a means of accessing neutral colors such as brown and black in electrochromic polymers.[8−12] With random copolymerization broad, low-energy (long wavelength) absorbances are often achieved by incorporating an electron-accepting moiety in the polymer backbone. The drawback of donor−acceptor systems is that they tend to have higher oxidation potentials caused by the accepting moiety, which limits optical memory (i.e., bistability) in the oxidized form, thus making their usefulness in devices limited. A new approach that circumvents the challenges caused by incorporating electron acceptors into the main chain is developed in this work. When considering how to make color tunable systems without acceptors, it is important to understand the design of materials for specific

regions of the color space (Figure 1a). All donor systems can cover three of the four regions shown here (wide, mid, and low gap), as green materials, having a highly negative $b*$, require dual absorption. The current state of the art all donor polymers were examined to develop an approach to make a color tunable system (Figure 1b).

Yellow ECPs, which utilize 1,4-phenylene linkages, have historically suffered from high oxidation potentials and low redox stability over 100 switches, which is attributed to the open sites on the aryl ring leaving the materials susceptible to nucleophilic attack or radical−radical coupling.[13,14] The incorporation of a dialkylthiophene (DAT) as a monomer of high redox stability in wide-gap electrochromic polymers has helped to overcome this challenge.[15] For absorbing the middle of the spectrum, the homopolymer of 3,4-propylenedioxythiophene (ProDOT) with 2-ethyl-hexyloxy side chains offers a high solubility and a low oxidation potential for switching as
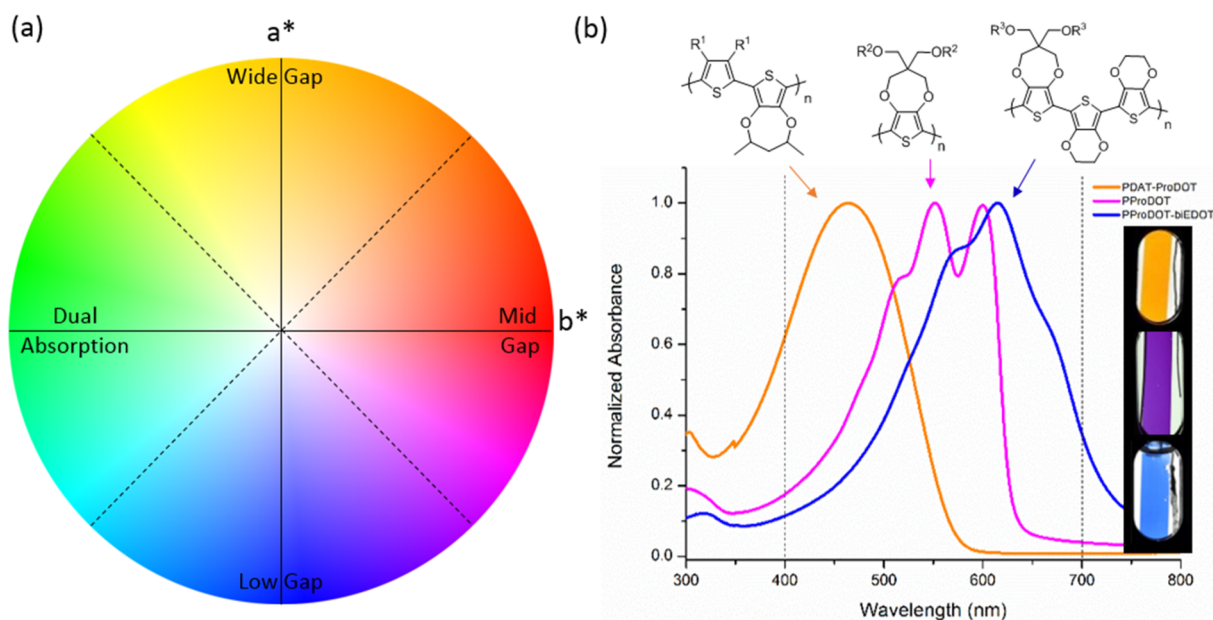

Figure 1. (a) $L*a*b*$ color space cross section and (b) all donor polymers used for inspiration that show tunability across the visible spectrum.
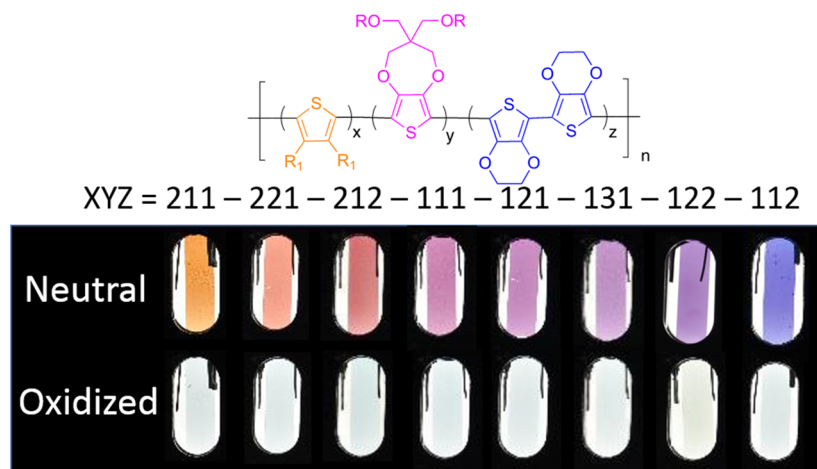

Figure 2. Repeat unit structure of random copolymers and target polymer ratios that allow access to an array of colors that span the visible spectrum and oxidize to transmissive forms.
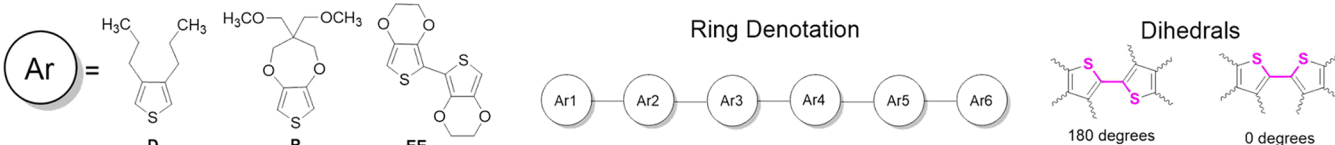
well as a high contrast.[16] This purple polymer also shows exemplary contrast, redox stability, and switching speed. For narrow-gap polymers, typically donor−acceptor systems are used. The drawbacks to these systems, as previously discussed, have been circumvented with the advent of a soluble poly(3,4-ethylenedioxythiophene) (PEDOT) analogue that covers the narrow-gap portion of the visible spectrum.[17] In this polymer, the biEDOT portion of the polymer brings electron richness and planarity, narrowing the optical gap and covering the low-energy portion of the visible region.

In this work, the combination of DAT, ProDOT, and biEDOT into random copolymers has been demonstrated to give broadly tunable electrochromic materials that span the visible spectrum (Figure 2). Using a tight feedback loop between theory and experiment, the ratios of these monomers are demonstrated to tune the absorbance of the resulting polymer, thus giving access to a wide range of colors in their neutral forms, while all being easily oxidized to highly transmissive states. Utilizing only these three monomers in different ratios provides access to polymers that are orange,

red, pink, magenta, purple, and blue, all of which can be oxidized to a highly transmissive form. Relative to the 1:1:1 ratio, an increased DAT content blue-shifts the absorbance of the polymer and an increased biEDOT content red-shifts the absorbance, while ProDOT brings a high solubility and a low oxidation potential. As detailed in Figure 2, the nomenclature of the polymers discussed in this work will be determined by the ratio of the monomers in the polymerization reaction. For example, a random copolymerization that is two parts DAT (x) and one part each ProDOT (y) and biEDOT (z) is **xyz211**.

RESULTS AND DISCUSSION

Quantum Chemical Calculations. To elucidate the impact on the number and identity of aryl ring incorporation on the color of these systems, density functional theory (DFT) is utilized. We have found that pairing the mPW1PBE functional with the cc-PVDZ basis set, while including dichloromethane through the conductor polarizable calculation model (CPCM), provides excellent correlation to experimental data.[18−21] A set of multiheterocycle oligomers is chosen to

Table 1. Calculated First Excited State Gaps, Dihedral Angles, and Visible Excited State Wavelengths and Oscillator Strengths for the Target Oligomers[a]

oligomer	E_g (eV)	dihedral angles					peak maximum	
		Ar1−Ar2	Ar2−Ar3	Ar3−Ar4	Ar4−Ar5	Ar5−Ar6	λ (nm)	f
PEEP	2.62	179.7	178.1	179.7			473.3	1.60
EEPEE	2.38	176.4	178.7	178.7	176.4		521.1	2.03
PEEPEE	2.22	179.3	177.9	179.0	179.7	178.5	559.6	2.48
DEED	2.72	156.9	179.7	156.9			456.6	1.54
EEDEE	2.45	178.3	168.4	168.4	178.3		506.4	1.94
EEPPEE	2.23	178.4	179.2	175.9	179.2	178.4	556.7	2.44
DPPD	3.09	46.8	175.6	48.9			401.3	1.27
PDPDP	2.49	169.1	176.9	176.9	169.1		497.4	1.79
PDEEDP	2.35	163.7	163.0	179.6	163.0	163.7	528.6	2.25
DPDP	2.98	137.2	160.9	136.9			416.2	1.19
DPDPD	2.48	178.6	179.9	179.9	178.6		500.8	1.90
DPDPDP	2.53	166.2	179.1	178.2	169.9	128.3	489.9	2.51

[a]The legend indicates how the structures and their corresponding dihedral angles are defined.

model possible random copolymers with varying degrees of conjugation and ring strain and to assess their influence on the predicted color (a complete list of the structures studied is given in Figure S1, and their calculated frontier molecular orbitals are provided in Figure S2). For each system, the neutral geometry is optimized followed by a frequency calculation to ensure the most stable configuration is produced. Time-dependent density functional theory (TD-DFT) calculations were then applied to these structures to simulate the ultraviolet−visible (UV−vis) spectra and predict the color of these oligomers.

An examination of the calculated HOMO−LUMO gaps provides direction with respect to the potential spectral breath, and the absorption tunability limits, which may be attained by the copolymers. As the strain along the backbone is increased by adding DAT units, the HOMO−LUMO gap is widened. Oligomers possessing the most DAT are particularly influenced by distortion from planarity causing a gap increase. The most twisted species (those that most deviate from the defined 180° antiplanar geometry) are DPPD, DPDP, DEED, and DPDPDP with values as low as 128.3°, 156.9°, 136.9°, and 46.8° and first excited state gaps of 3.09, 2.98, 2.72, and 2.53 eV, respectively (see Table 1). DPDPDP is the only 6-aryl group oligomer to be greatly impacted by inclusion of DAT as compared to PDEEDP, which possesses a first excited state gap that is nearly 0.2 eV smaller. The remaining oligomers demonstrate that, as the conjugation is extended, the first excited state gap is reduced as seen in EEPPEE and PEEPEE.

The calculated UV−vis spectra of these systems provide visible peak maxima that vary from 401 to 560 nm, spanning a difference of nearly 160 nm. Of the 15 generated excited states, only three or four possess oscillator strengths of ≥0.1 (see Table S1). This observation shows that the absorptions are dominated by a small number of optical transitions of significance. Aside from the locations of the peak maxima, there are no differences in the predicted peak shapes in the visible range as shown in Figure 3 (for more detailed comparisons, see Figures S3 and S4). In fact, members of
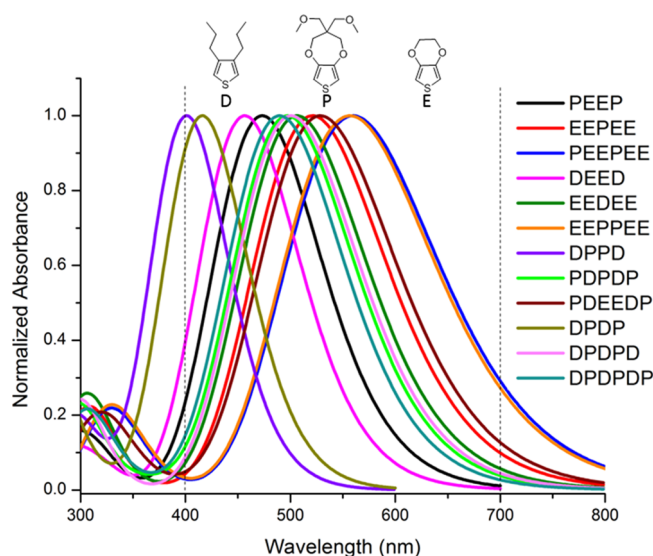

Figure 3. Calculated UV−vis−NIR absorbance of the model chromophores showing the limits of spectral breadth accessible for this approach. The side chains for each monomer have been reduced to avoid local energy minima caused by many degrees of free rotation of the alkyl chains.

the set of oligomers possessing five aryl groups produce nearly identical spectra and have peak maxima that differ by only 24 nm. The four- and six-aryl group structures are more impacted by torsion along the backbone and have ranges of 72 and 70 nm, respectively.

The simulated UV−vis spectra of these molecules also provide a means of estimating the color that may be produced in the CIE L*a*b* color space.[22−24] Positive a* and b* values represent red and yellow, respectively, while the negative values indicate blue and green, respectively. As the magnitudes of a* and b* increase, the color becomes more saturated, and as one traverses between color points, the hue changes. L* depicts the lightness: a value of 0 would be black, and a value
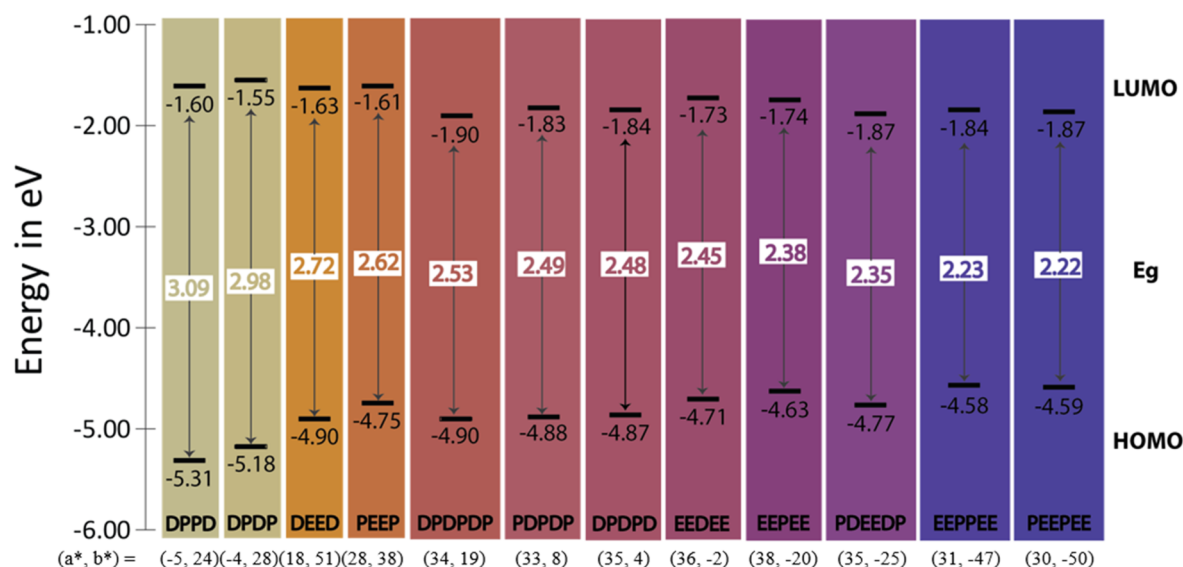
Figure 4. Corresponding HOMO, LUMO, and first excited state gaps are provided for the calculated oligomers. They are arranged in order of decreasing first excited state gap. The RGB color is provided as for each data set, and the corresponding ($a*$ and $b*$) values are given below the corresponding energy level diagram.

Scheme 1. Synthetic Approach to Random Copolymerization through Direct Arylation
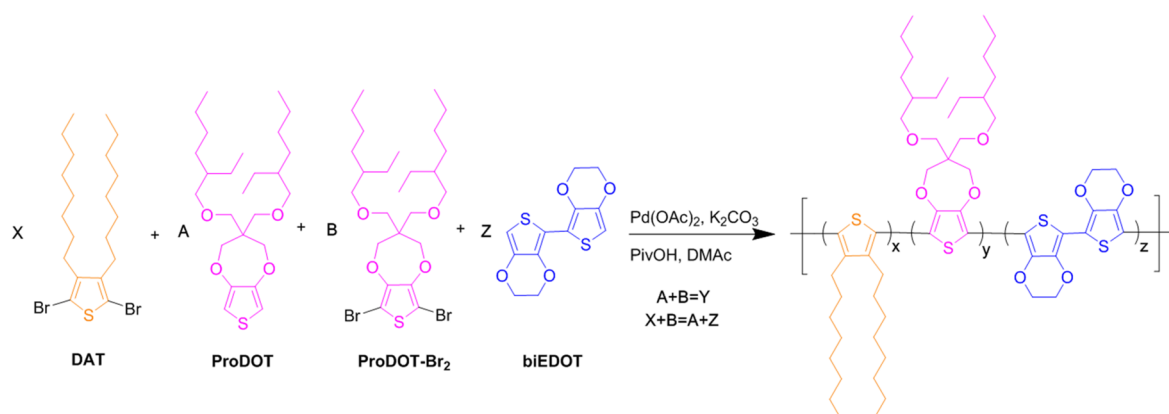
of 100 would be white. The $L*$, $a*$, and $b*$ coordinates are translated to the RGB color space to display the predicted color of the oligomers (both sets of coordinates are listed in Table S2) and are indicated in Figure 4 along with their corresponding HOMO, LUMO, and first excited state gap values. The predicted colors give a range of the color space that could be reached experimentally and show that these monomers have the potential to cover wide-gap, midgap, and narrow-gap absorptions.

Polymer Synthesis and Characterization. The approach to the polymer syntheses is shown in Scheme 1. The polymers were prepared via direct (hetero)arylation polymerization where the ratios of the monomers allow for tuning the color. The stoichiometry is balanced by using the proper proportions of ProDOT and ProDOT-Br₂ such that the aryl bond carbon–bromide:carbon–hydrogen ratio is equal to 1. The polymerizations were carried out under an argon atmosphere over 24 h followed by precipitation into methanol, followed by purification via Soxhlet extraction, during which they were washed with methanol, acetone, hexanes, and chloroform. The chloroform fraction was retained and underwent palladium and potassium scavenging before being reprecipitated, filtered, and dried to afford the desired product.

Polymerization yields were all ≥67%, and GPC-estimated molecular weights were all ≥10 kDa, relative to a polystyrene standard. These molecular weights show that the polymers are above the effective conjugation length and would not undergo a change in color if they were longer. Polymerization yields and GPC-estimated molecular weights are collated in Table 2, and all GPC traces are shown in Figure S5. As one can see by the elemental analysis results, the polymers tend to have high sulfur percentages and low carbon and hydrogen percentages.

Table 2. GPC-Estimated Polymer Molecular Weights and Polymerization Yields

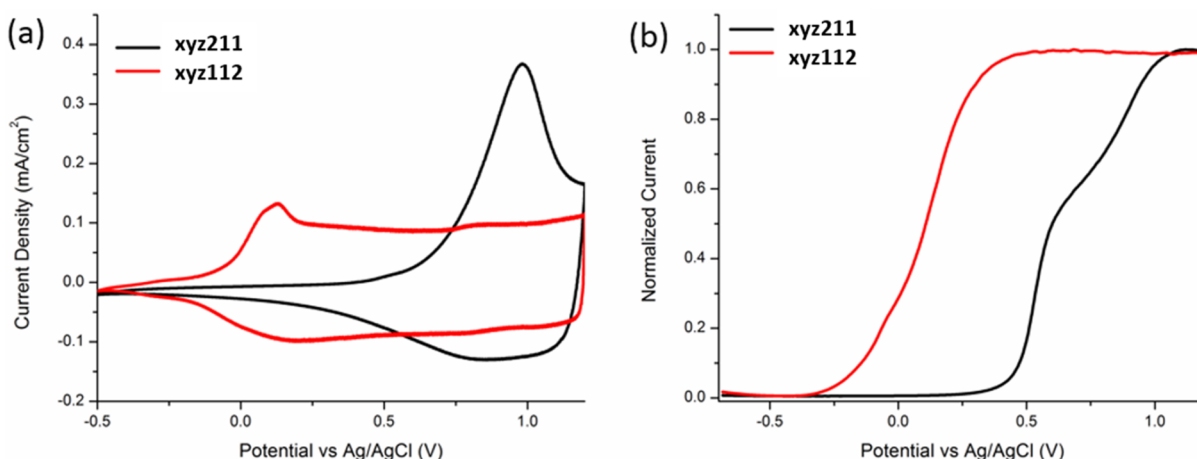| polymer	yield (%)	M_n (kDa)	Đ
xyz211	77	13	1.4
xyz221	72	33	2.0
xyz212	69	15	1.8
xyz111	75	22	2.4
xyz121	81	26	3.4
xyz131	69	17	2.3
xyz122	67	15	1.7
xyz112	70	10	1.5

Figure 5. Comparison of (a) CV and (b) DPV of **xyz211** and **xyz112** on a Pt button electrode in 0.5 M TBAPF$_6$/PC. Reference: 450 mV vs Fc/Fc$^+$.

This is indicative of incorporation of more biEDOT into the structure compared to what the monomer feed ratio would suggest. This is can be explained by the relative reactivity and solubility of the monomers. DAT is less reactive and is incorporated into the copolymer at a rate slower than that of biEDOT, so there is significant copolymer drift early in the polymerization. As more biEDOT is added to the polymer, the polymer becomes less soluble due to the lack of side chains present in the monomer. This leads to polymers with the most biEDOT to precipitate from the polymerization and thus incorporate less DAT and ProDOT into the structure. Synthetic procedures, nuclear magnetic resonance spectra, and elemental analyses are also given in the Supporting Information. All polymers are soluble in CHCl$_3$ upward of 5 mg/mL allowing for airbrush spray processing and drop casting for film formation.

Electrochemical and Optical Properties. For electrochemical characterization, polymer films are drop cast onto Pt button electrodes from 2 mg/mL solutions (3 μL) in CHCl$_3$ to cover the electrode. Cyclic voltammetry (CV) and differential pulse voltammetry (DPV) were performed on films of the polymers to gain insight into how the different comonomers affected the electrochemical properties of the resulting polymers. Representative CV and DPV data are provided in Figure 5 for **xyz211** and **xyz112**. Upon examination of the electrochemical oxidation of the materials via DPV, the onset of oxidation follows the expected trend of polymers containing more DAT having higher oxidation potentials (CV and DPV data for polymers can be found in Figure S6). As monomer ratios are tuned, the resultant onsets of oxidation (E_{ox}), as determined by DPV, range from −81 to 476 mV relative to Ag/AgCl giving a large window for tuning the desired electrochemical switching potential (E_{ox} values are listed in Table 3).

The E_{ox} for **xyz111** was found at 141 mV, and as more DAT is added to the polymer structure, the E_{ox} increases. **xyz221** has an E_{ox} of 444 mV, and the highest E_{ox} was found for **xyz211** (476 mV). This observation is due to DAT being the least electron rich of the monomers and also providing the most interring strain. More interring strain causes a higher energy barrier to planarize the conjugated backbone upon oxidation. Conversely, biEDOT provides more planarity and electron richness to the polymer compared to DAT; thus, increasing the ratio of biEDOT in the structure lowers the oxidation

Table 3. Optical and Electrochemical Properties of Studied ECPs

polymer	E_{ox}[a] (mV) vs Ag/AgCl	λ_{max} (nm)[b]	E_g[b,c] (eV)
xyz211	476	458	2.04
xyz221	444	495	1.88
xyz212	163	512	1.83
xyz111	141	539	1.82
xyz121	101	550	1.81
xyz131	105	553	1.77
xyz122	−46	568	1.75
xyz112	−81	586	1.70

[a]As determined by DPV as the onset of the current for oxidation. [b]For films cast onto ITO-coated glass measured after 10 CV cycles. [c]Bandgap determined by the onset of light absorption.

potential. This is seen in **xyz122** having an E_{ox} of −46 mV and **xyz112** being the polymer with the lowest E_{ox} (−81 mV).

For optical characterization, polymer films were airbrush sprayed onto glass/ITO electrodes from 3 mg/mL solutions in 1:1 toluene/chloroform mixtures. All of the polymers form smooth films with little scattering. Films are sprayed to an absorbance of 1.00 ± 0.05 in the as-cast state. UV−vis spectra are measured in a 0.5 M TBAPF$_6$/PC electrolyte solution after 10 CV cycles, as the polymers swell with electrolyte upon oxidation and their absorbance intensities and λ_{max} may change. Upon electrochemical conditioning of electrochromic polymers in general, the UV−vis absorption typically exhibits a characteristic red-shift of the absorbance as the polymer's conjugation in the charge neutral state is extended compared to that of the as-cast film. Absorbance values are normalized due to the increase or decrease in absorbance upon redox cycling. Figure 6 shows the UV−vis spectra of the films of the polymers after break-in. These polymers' absorptions show a range of λ_{max} from 458 to 586 nm and optical gaps (E_g) from 1.70 to 2.04 eV, which covers a large portion of the visible spectrum.

Using **xyz111** as a reference point for each case, the λ_{max} is 539 nm and the E_g is 1.82 eV. It is evident that the amount of DAT in the polymer has a profound effect on both the λ_{max} and the E_g, as evidenced in Figure 6a. This monomer causes the most interring strain, so for every DAT inserted into the backbone there is a point of torsion that decreases π−π overlap between rings, decreasing the effective conjugation length and
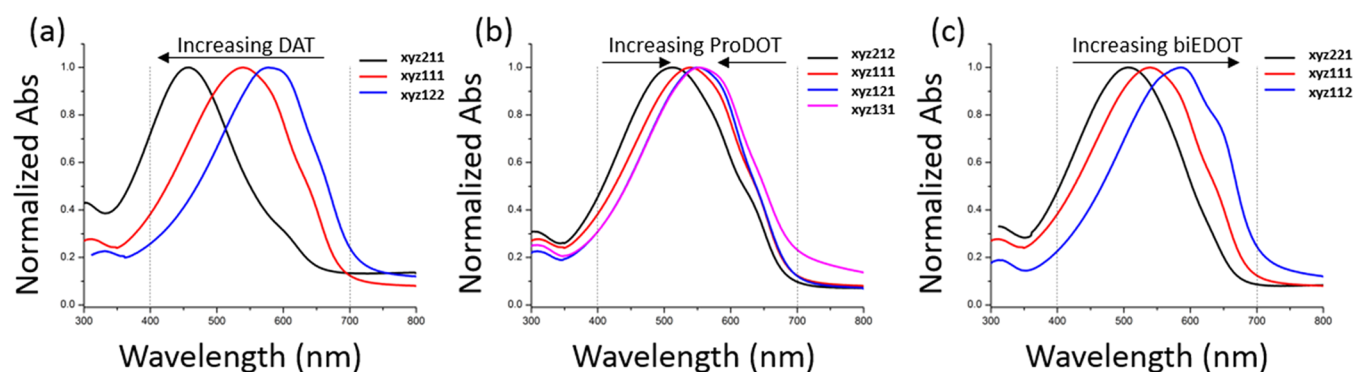
Figure 6. Neutral state spectra on ITO-coated glass comparing the effects of varying the amount of (a) DAT, (b) ProDOT, and (c) biEDOT while holding the ratios of the other monomer constant.
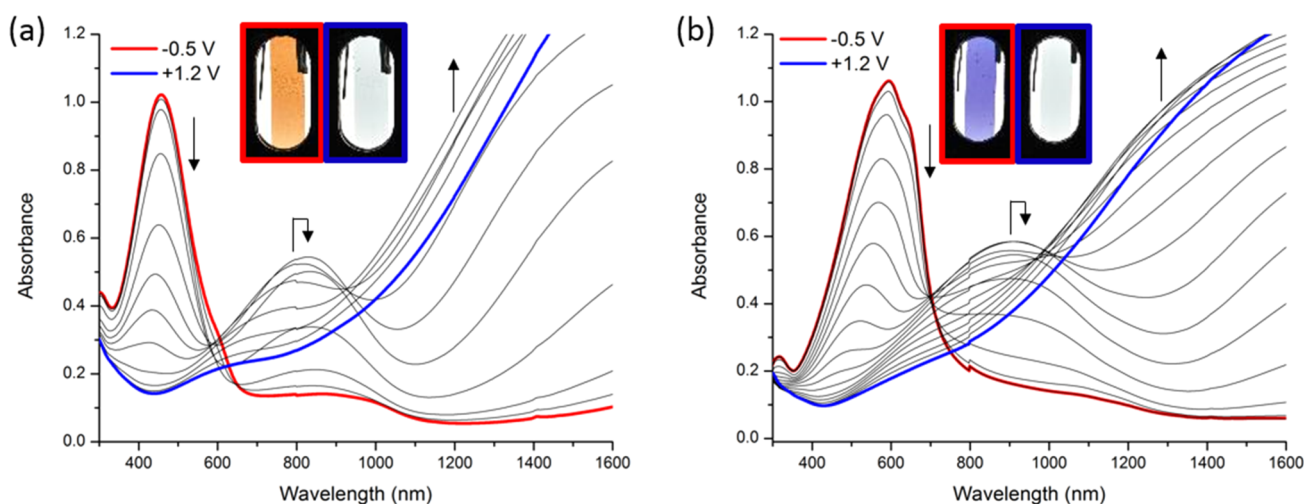

Figure 7. Spectroelectrochemistry and photographs of (a) **xyz211** and (b) **xyz112**. The applied potential was increased in 100 mV steps between the fully colored and bleached states in 0.5 M TBAPF$_6$/PC.

widening the optical gap. With **xyz211** having the highest ratio of DAT, it has the highest energy and broadest absorption with the λ_{max} at 458 nm and an E_g of 2.04 eV. As the DAT content is reduced compared to that of **xyz111**, there is a red-shifting in the λ_{max} to 568 nm and a narrowing of the peak to give an E_g of 1.75 eV for **xyz122**.

The ratio of biEDOT has an analogous, but opposite, trend compared to that observed for DAT (Figure 6c). As the biEDOT ratio is increased, there is a red-shifting of the λ_{max} to 495, 539, and 586 nm for **xyz221**, **xyz111**, and **xyz112**, respectively. The E_g as a function of biEDOT content also shows an analogous and opposite trend compared to that of DAT, where there is a decrease in E_g as the biEDOT ratio is increased from 1.88 eV for **xyz221** to 1.70 eV for **xyz112**.

The ProDOT content has the smallest effect on controlling the absorption (Figure 6b), which is expected because its contribution to visible light absorption lies between those of the other monomers in terms of electron richness and interring planarity. As the ProDOT ratio is increased, there is a red-shifting of the λ_{max} to 512, 539, 550, and 553 nm for **xyz212**, **xyz111**, **xyz121**, and **xyz131**, respectively. The high-energy absorption of **xyz212** is likely due to the high content of DAT, and as the ProDOT content is further increased, there is a smaller red-shifting effect, such as the small 3 nm shift between **xyz121** and **xyz131**. A similar trend is also seen when examining the E_g as a function of ProDOT content. As the

amount of ProDOT is increased, there is a small range in the E_g from 1.83 eV for **xyz212** to 1.77 eV for **xyz131**. By this point, the optical properties of the polymer are dominated by the ProDOT repeat units.

Color and Switching Properties. Spectroelectrochemical measurements were performed on polymer films sprayed on ITO glass in 0.5 M TBAPF$_6$/PC with a platinum counter electrode and a Ag/AgCl reference electrode. Representative results for **xyz211** and **xyz112** are detailed in Figure 7 along with photographs of the films held at potential extremes dictated by the CV results (spectroelectrochemistry results for all polymers are shown in Figures S7 and S8). In these experiments, a three-electrode cell is set up in a cuvette where the polymer film cast on ITO acts as the working electrode. The UV−vis spectrum is then monitored as a function of the potential applied to the film. As one can see in the figure, the neutral state absorption in the visible region is depleted upon oxidation, and there is an increase in the charged state absorption in the near infrared. After complete oxidation, all of the polymers show high transmissivity across the visible range. This transition between colored and transmissive can also be observed in the photography. A chronoabsorptometry experiment was carried out to show the contrast of the polymers as a function of switching speed and repeated switching (Figures S9 and S10). In this experiment, the transmittance at λ_{max} is monitored as the films are oxidized and reduced at varying

frequencies. This experiment demonstrates that these polymers can undergo repeated switching while maintaining their optical contrast.

In this work, the color is quantified using the $L^*a^*b^*$ color space. Colorimetry is used to demonstrate the control over color with this material design approach. The a^*b^* color space results for the polymer films are presented graphically in Figure 8 with the $L^*a^*b^*$ values listed in Table 4. In this figure, the
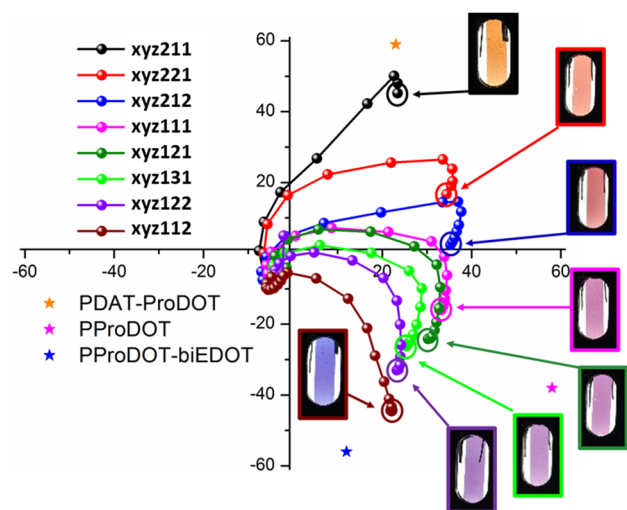

Figure 8. Colorimetric analysis and neutral state photographs of all of the polymers. Plots of a^*b^* color coordinates at increasing applied potentials in 0.1 V steps from neutral (-0.5 V vs Ag/AgCl) to fully oxidized states (1.2 V vs Ag/AgCl). Measurements were performed in 0.5 M TBAPF$_6$/PC of films spray-cast onto ITO/glass electrodes.

Table 4. Color and Switching Properties of All Donor Random Electrochromic Polymers

polymer	$\Delta\%T^{a,b}$ (at λ_{max})	neutral state L^*, a^*, b^* color coordinates[b]	oxidized state L^*, a^*, b^* color coordinates[b]
xyz211	62	66, 23, 45	84, -2, -6
xyz221	70	62, 34, 16	91, -2, -7
xyz212	67	44, 35, 2	86, -2, -6
xyz111	64	40, 33, -16	87, -2, -5
xyz121	66	47, 30, -24	90, -1, -4
xyz131	62	46, 25, -26	89, -3, -5
xyz122	60	42, 23, -33	88, -2, -5
xyz112	58	32, 22, -44	88, -2, -6
PDAT-ProDOT[c]	65	87, 23, 59	90, -2, -4
PProDOT[c]	71	42, 58, -38	89, -3, -3
PProDOT-biEDOT[c]	71	34, 10, -56	83, -3, -5

[a]Difference between transmittance measured in fully oxidized and fully neutral states (all films sprayed to 10%T at λ_{max}). [b]For a film cast onto ITO-coated glass. [c]Values from refs 15 and 17.

polymer neutral states are circled and lines are used to guide the eye between the 100 mV spaced measurement points. Neutral state colorimetry values are provided as stars for the homopolymer PProDOT and two alternating polymers PDAT-ProDOT and PProDOT-biEDOT in Figure 8 for comparison. It is apparent that all of these new random copolymers are less saturated than the polymers with the more regular repeat units, as they are broader in absorbance. In the neutral state, after a redox switching equilibration, the polymers had L^* values

ranging from 32 to 66, a^* values ranging from 22 to 35, and b^* values ranging from -44 to 45, thus traversing the wide-gap, midgap, and low-gap color spaces mentioned in Figure 1a. In the oxidized states, the polymers exhibited high L^* values ranging from 86 to 91 coupled with low a^* values ranging from -3 to -1 and b^* values ranging from -7 to -4, thus giving forms that are both highly transmissive and color neutral.

Taking a closer look at the "hurricane-like" tracking analysis for all of the polymer films, we find an observed initial increase in b^* as the film begins to be oxidized. As the polymers are random in repeat pattern, the individual chromophores along the chain will have varying oxidation potentials, where those with the lowest oxidation potential contain the most DOT and least DAT and would, therefore, have the most red-shifted (blue light transmitting) absorptions. As the polymer is oxidized, these chromophores are oxidized first, leaving the highest oxidation potential and widest-gap chromophores, consisting of the portions with the most DAT incorporated into the chain, in their neutral form. The polymers with the most DOT in their structure have more gradual increases in b^* as they begin to oxidize, while the polymers with the least DOT have small sharp jumps in b^* at the beginning of oxidation.

Upon examination of the breadth of the color space that can be obtained through this approach, the most logical reference point is the polymer containing equal parts of each monomer. The neutral state for **xyz111** has a^* and b^* values of 33 and -16, respectively, which is observed as a purple-pink color in the photography. As more ProDOT is added to the structure, there is a decrease in the a^* and b^* values for **xyz121** (30 and -24, respectively), which continues to **xyz131** (25 and 26, respectively). This shift in values is indicative of a stronger blue hue, and a decrease in the red hue of the film, which is observed in the photography as the films appearing less pink and more purple relative to **xyz111**. As more biEDOT is added to the polymer structures, there is less interring strain, further red-shifting absorbance, and more blue light is transmitted. For **xyz122** (23 and -33, respectively) and **xyz112** (22 and -44, respectively), there is a large decrease in b^* values leading to very blue-colored films seen in the photography. Similar to the electrochemistry, the incorporation of DAT has the largest effect on the colorimetry. As more DAT is added to the structure, there is more interring strain, further blue-shifting absorbance, and more red light is transmitted. This causes an increase in the b^* value, indicating that the color is becoming less blue. The colorimetry values for **xyz212** (35 and 2, respectively) are near the positive a^* axis, observed as a red color in the photography. Replacing the biEDOT with the slightly more strained ProDOT in **xyz221** (34 and 16, respectively) leads to an increase in a^* values leading to light red film. For **xyz211** (23 and 45, respectively), there is a large increase in a^* values, as the polymer structure is dominated by the high-strain monomer, leading to an orange film. With this, it is evident that a broad portion of color space, from the low-gap region through the midgap region and into the high-gap region, can be accessed with three simple repeat units randomly distributed along the chain.

Color Mixing. To demonstrate how we can expand the spectral and color range accessible by these ECPs, two of these polymers were combined in different ratios to create broadly absorbing blends (Figure 9). In this experiment, solution mixtures of **xyz211** and **xyz112** at 3 mg/mL were mixed in ratios of 1:1 and 2:1 and films were cast via airbrush spraying.
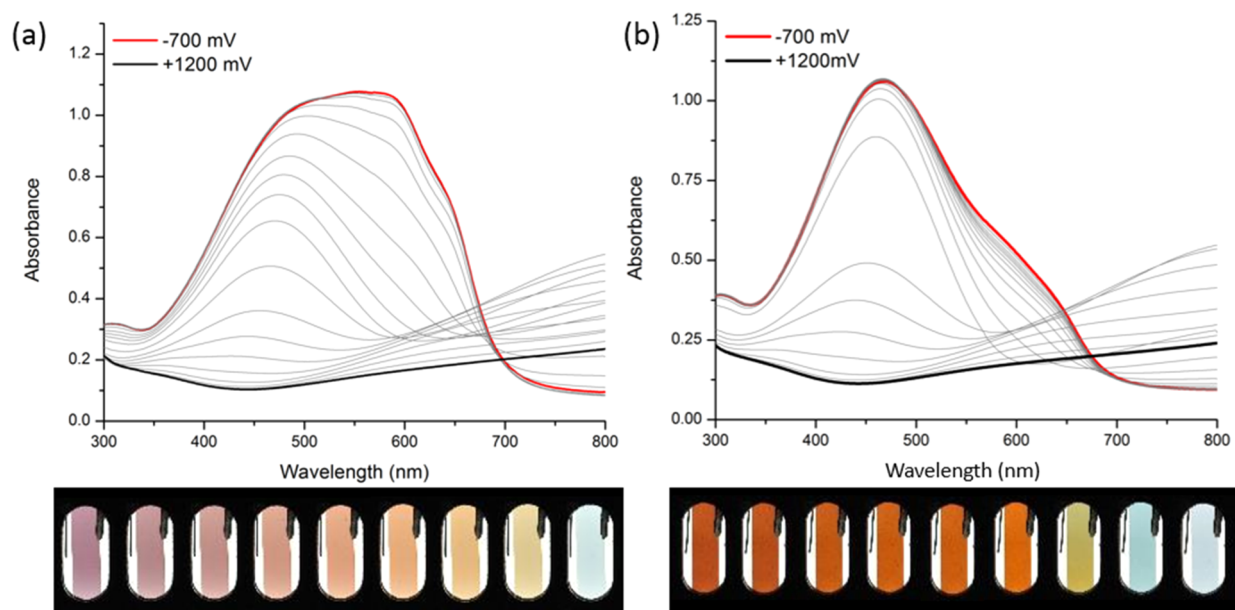
Figure 9. Spectroelectrochemistry and photography of mixtures of **xyz211** and **xyz122** at ratios of (a) 1:1 and (b) 2:1. The applied potential was increased in 100 mV steps between the fully colored and bleached states in 0.5 M TBAPF$_6$/PC. The photographs were taken from −600 to 1000 mV in 200 mV steps to show the progression of the color change as a function of applied potential.

The spectroelectrochemical and photographic results show the potential for solution phase color mixing of these polymers, similar to inks, to create films of low color saturation, which are of interest for eyewear and tinting applications.[25,26] The limitations of this all donor approach to creating black-to-clear switching electrochromics are evident in Figure 9a. This 1:1 mixture of polymers gives a conformal absorption between ∼450 and ∼650 nm, but some red and blue light transmit at the peripheries of the visible range causing the material to appear purple. Without the donor−acceptor interaction that is commonly used to synthesize low-gap conjugated polymers that can absorb well into the near-infrared region, a full absorption across the visible spectrum is not feasible. In general, randomly distributed chromophore black and brown ECPs containing donor−acceptor moieties also provide a challenge where the portion of the chain with the largest donor content bleaches well before the other portions, leaving a green intermediate state that is not desirable for eyewear and tinting applications.

As shown in Figure 9b, the 2:1 ratio of **xyz211** and **xyz112** affords an aesthetically pleasing orange/brown-to-transmissive switching blend, albeit with a golden intermediate color, prior to the transition to the light blue transmissive form. Considering eyewear and tinting applications of electrochromism, complex colors that include browns and various shades of red that can be attained through the mixing process are desirable.

CONCLUSION

Electrochromism is a field where small changes in color can have large ramifications on the applicability of the material into devices. In this work, a tight feedback loop of calculations and experiments guided the design of randomly structured electrochromic polymers with internal chromophores that cover most of the visible spectrum with only three monomer repeat units. TDDFT was used to predict the spectral breadth that could be attained with these systems and guided the

synthesis. The synthesized materials allowed for a large portion of the low-, mid-, and high-gap color space to be covered while maintaining low oxidation potentials, high contrast, and long-lasting optical memory. These properties allow the materials to function with a low level of power consumption as desired for systems with portable (e.g., battery) power supplies. Their mixture and subsequent processing into broadly absorbing blends have potential in applications where muted and secondary colors are beneficial.

ASSOCIATED CONTENT

Ⓢ Supporting Information

The Supporting Information is available free of charge on the ACS Publications website at DOI: 10.1021/acs.chemmater.9b01293.

> Supplementary figures, including details about the calculations and characterization for all polymers using gel permeation chromatography, cyclic voltammetry, differential pulse voltammetry, spectroelectrochemistry, and kinetic switching; experimental details; synthetic procedures; and primary characterizations (PDF)

AUTHOR INFORMATION

Corresponding Author
*E-mail: reynolds@chemistry.gatech.edu.

ORCID Ⓞ
Dylan T. Christiansen: 0000-0002-8673-5870
Shunsuke Ohtani: 0000-0002-8669-1089
John R. Reynolds: 0000-0002-7417-4869

Notes
The authors declare the following competing financial interest(s): Electrochromic polymer technology developed at the Georgia Institute of Technology has been licensed to NXN Licensing. J.R.R. serves as a consultant to NXN Licensing.

■ ACKNOWLEDGMENTS

■ REFERENCES

(1) Dyer, A. L.; Thompson, E. J.; Reynolds, J. R. Completing the Color Palette with Spray-Processable Polymer Electrochromics. *ACS Appl. Mater. Interfaces* **2011**, *3* (6), 1787−1795.

(2) Yen, H. J.; Chen, C. J.; Liou, G. S. Flexible Multi-Colored Electrochromic and Volatile Polymer Memory Devices Derived from Starburst Triarylamine-Based Electroactive Polyimide. *Adv. Funct. Mater.* **2013**, *23* (42), 5307−5316.

(3) Sönmez, G.; Schwendeman, I.; Schottland, P.; Zong, K.; Reynolds, J. R. N-Substituted Poly(3,4-Propylenedioxypyrrole)s: High Gap and Low Redox Potential Switching Electroactive and Electrochromic Polymers. *Macromolecules* **2003**, *36* (3), 639−647.

(4) Özkut, M. I.; Algi, M. P.; Öztaş, Z.; Algi, F.; Önal, A. M.; Cihaner, A. Members of CMY Color Space: Cyan and Magenta Colored Polymers Based on Oxadiazole Acceptor Unit. *Macromolecules* **2012**, *45* (2), 729−734.

(5) Sonmez, G.; Sonmez, H. B.; Shen, C. K. F.; Jost, R. W.; Rubin, Y.; Wudl, F. A Processable Green Polymeric Electrochromic. *Macromolecules* **2005**, *38* (3), 669−675.

(6) Yen, H.-J.; Liou, G.-S. Solution-Processable Triarylamine-Based Electroactive High Performance Polymers for Anodically Electrochromic Applications. *Polym. Chem.* **2012**, *3* (2), 255−264.

(7) İçli, M.; Pamuk, M.; Algi, F.; Önal, A. M.; Cihaner, A. Donor−Acceptor Polymer Electrochromes with Tunable Colors and Performance. *Chem. Mater.* **2010**, *22* (13), 4034−4044.

(8) Shi, P.; Amb, C. M.; Knott, E. P.; Thompson, E. J.; Liu, D. Y.; Mei, J.; Dyer, A. L.; Reynolds, J. R. Broadly Absorbing Black to Transmissive Switching Electrochromic Polymers. *Adv. Mater.* **2010**, *22* (44), 4949−4953.

(9) Yen, H.-J.; Lin, K.-Y.; Liou, G.-S. Transmissive to Black Electrochromic Aramids with High Near-Infrared and Multicolor Electrochromism Based on Electroactive Tetraphenylbenzidine Units. *J. Mater. Chem.* **2011**, *21* (17), 6230−6237.

(10) Xu, L.; Zhao, J.; Cui, C.; Liu, R.; Liu, J.; Wang, H. Electrosynthesis and Characterization of an Electrochromic Material from Poly (1, 4-Bis (2-Thienyl)-Benzene) and Its Application in Electrochromic Devices. *Electrochim. Acta* **2011**, *56* (7), 2815−2822.

(11) Xu, Z.; Chen, X.; Mi, S.; Zheng, J.; Xu, C. Solution-Processable Electrochromic Red-to-Transmissive Polymers with Tunable Neutral State Colors, High Contrast and Enhanced Stability. *Org. Electron.* **2015**, *26*, 129−136.

(12) Lee, J. Y.; Han, S.-Y.; Lim, B.; Nah, Y.-C. A Novel Quinoxaline-Based Donor-Acceptor Type Electrochromic Polymer. *J. Ind. Eng. Chem.* **2019**, *70*, 380−384.

(13) Kerszulis, J. A.; Amb, C. M.; Dyer, A. L.; Reynolds, J. R. Follow the Yellow Brick Road: Structural Optimization of Vibrant Yellow-to-Transmissive Electrochromic Conjugated Polymers. *Macromolecules* **2014**, *47* (16), 5462−5469.

(14) Cao, K.; Shen, D. E.; Österholm, A. M.; Kerszulis, J. A.; Reynolds, J. R. Tuning Color, Contrast, and Redox Stability in High Gap Cathodically Coloring Electrochromic Polymers. *Macromolecules* **2016**, *49* (22), 8498−8507.

(15) Christiansen, D. T.; Reynolds, J. R. A Fruitful Usage of a Dialkylthiophene Comonomer for Redox Stable Wide-Gap Cathodically Coloring Electrochromic Polymers. *Macromolecules* **2018**, *51* (22), 9250−9258.

(16) Reeves, B. D.; Grenier, C. R. G.; Argun, A. A.; Cirpan, A.; McCarley, T. D.; Reynolds, J. R. Spray Coatable Electrochromic Dioxythiophene Polymers with High Coloration Efficiencies. *Macromolecules* **2004**, *37* (20), 7559−7569.

(17) Ponder, J. F., Jr; Österholm, A. M.; Reynolds, J. R. Designing a Soluble PEDOT Analogue without Surfactants or Dispersants. *Macromolecules* **2016**, *49* (6), 2106−2111.

(18) Barone, V.; Cossi, M. Quantum Calculation of Molecular Energies and Energy Gradients in Solution by a Conductor Solvent Model. *J. Phys. Chem. A* **1998**, *102* (11), 1995−2001.

(19) Cossi, M.; Rega, N.; Scalmani, G.; Barone, V. Energies, Structures, and Electronic Properties of Molecules in Solution with the C-PCM Solvation Model. *J. Comput. Chem.* **2003**, *24* (6), 669−681.

(20) Wheeler, D. L.; Rainwater, L. E.; Green, A. R.; Tomlinson, A. L. Modeling Electrochromic Poly-Dioxythiophene-Containing Materials through TDDFT. *Phys. Chem. Chem. Phys.* **2017**, *19* (30), 20251−20258.

(21) Christiansen, D. T.; Wheeler, D. L.; Tomlinson, A. L.; Reynolds, J. R. Electrochromism of Alkylene-Linked Discrete Chromophore Polymers with Broad Radical Cation Light Absorption. *Polym. Chem.* **2018**, *9*, 3055−3066.

(22) Mortimer, R. J.; Varley, T. S. Quantification of Colour Stimuli through the Calculation of CIE Chromaticity Coordinates and Luminance Data for Application to Insitu Colorimetry Studies of Electrochromic Materials. *Displays* **2011**, *32* (1), 35−44.

(23) McLaren, K. XIII—The Development of the CIE 1976 (L* A* B*) Uniform Colour Space and Colour-difference Formula. *J. Soc. Dyers Colour.* **1976**, *92* (9), 338−341.

(24) Robertson, A. R. The CIE 1976 Color-difference Formulae. *Color Res. Appl.* **1977**, *2* (1), 7−11.

(25) Bulloch, R. H.; Kerszulis, J. A.; Dyer, A. L.; Reynolds, J. R. An Electrochromic Painter's Palette: Color Mixing via Solution Co-Processing. *ACS Appl. Mater. Interfaces* **2015**, *7*, 1406−1412.

(26) Österholm, A. M.; Shen, D. E.; Kerszulis, J. A.; Bulloch, R. H.; Kuepfert, M.; Dyer, A. L.; Reynolds, J. R. Four Shades of Brown: Tuning of Electrochromic Polymer Blends toward High-Contrast Eyewear. *ACS Appl. Mater. Interfaces* **2015**, *7* (3), 1413−1421.